

Revisiting Power Systems Time-domain Simulation Methods and Models

Jose Daniel Lara, *Member, IEEE*, Rodrigo Henriquez-Auba, *Member, IEEE*,
Deepak Ramasubramanian, *Senior Member, IEEE*, Sairaj Dhople, *Senior Member, IEEE*,
Duncan S. Callaway, *Member, IEEE* and Seth Sanders, *Fellow Member, IEEE*

Abstract—The changing nature of power systems dynamics is challenging present practices related to modeling and study of system-level dynamic behavior. While developing new techniques and models to handle the new modeling requirements, it is also critical to review some of the terminology used to describe existing simulation approaches and the embedded assumptions. This paper provides a first-principles review of the *simplifications and transformations* commonly used in the formulation of time-domain simulation models. It introduces a taxonomy and classification of time-domain simulation models depending on their frequency bandwidth, network representation, and software availability. Furthermore, it focuses on the fundamental aspects of averaging techniques, and model reduction approaches that result in modeling choices, and discusses the associated challenges and opportunities of applying these methods in systems with large shares of Inverter Based Resources (IBRs). The paper concludes with an illustrative simulation that compares the trajectories of an IBR-dominated system.

Index Terms—Modeling, Power system analysis, Simulation

I. INTRODUCTION

THE increasing integration of generation sources via power electronics is changing power systems. It is generally agreed that new dynamics in the controls of Inverter-based Resources (IBRs) change modeling requirements for system-wide stability studies that rely on time-domain simulations [1]–[3]. In power systems dominated by synchronous generators, physical phenomena (magnetic fluxes, electromechanics, mechanical control reaction times, or thermodynamic processes) drive dynamic behavior. The control logic associated with synchronous generators is commonly tuned to the timescale of the relevant processes, creating a *natural* separation between the dynamic behaviors attributable to physics

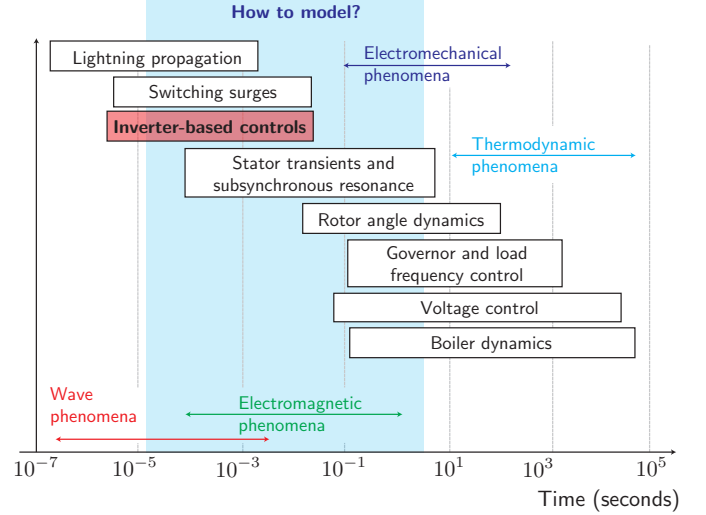


Fig. 1. Time scales for power systems dynamic behavior. Synchronous machine-dominated systems exhibit dynamics dominated by physical laws. IBRs introduces new dynamics from logical components and pose new challenges in simulation model complexity for time-domain simulations [2].

and controls. On the other hand, IBR dynamics are dominated by their controls, including modulation, Phase-locked Loops (PLLs), voltage, current, and power controllers. Therefore, the practical requirements of control design—often cascading PID control—defines the relationships between timescales. In fact, interactions at higher frequencies have recently been recognized with a new stability category [2], highlighting the exigent need to revisit our understanding of system dynamics with high penetrations of IBRs. The main goal of a time-domain simulation is to determine if there is a bounded trajectory of the system towards an equilibrium point following a disturbance. Determining the level of modeling detail required to capture the particular phenomena of interest accurately is key when developing a power systems simulation model.

Figure 1 shows the classification of power systems dynamic behaviors, as presented in [2], and highlights the timescales over which IBRs interact with both electromechanical and electromagnetic phenomena. Further, the modeling choices determine the algorithmic and computational requirements to execute the time-domain simulation since analytical approaches do not typically scale for system-level studies. In systems supplied predominantly by synchronous generators, IEEE Std 1110-2019 [4] guides the generator model complexity requirements based on the stability category under study and the

Corresponding author: jdlara@berkeley.edu

This research was supported by the U.S. Department of Energy by the Advanced Grid Modeling program within the Office of Electricity, under contract DE-AC02-05CH1123, and by the Solar Energy Technologies Office through award 38637 (UNIFI Consortium). The views expressed herein do not necessarily represent the views of the U.S. Department of Energy or the United States Government.

J. D. Lara and D. S. Callaway are with the Energy and Resources Group at the University of California Berkeley.

R. Henriquez-Auba, D. S. Callaway and S. Sanders are with the Department of Electrical Engineering and Computer Sciences at the University of California Berkeley.

J. D. Lara and R. Henriquez-Auba are also with the National Renewable Energy Laboratory, Golden, Colorado.

D. Ramasubramanian is with the Electric Power Research Institute, Knoxville, Tennessee.

S. Dhople is with the Department of Electrical Engineering at University of Minnesota.

Manuscript received April 19, 2005; revised August 26, 2015.

severity of the perturbation. However, up to now, no such modeling guidance exists for IBR dominated systems.

Several earlier papers have explored the modeling requirements for systems with IBRs and shed light on the theoretical [5]–[7] and practical [8] requirements for time-domain simulation of large systems, particularly concerning the modeling of network circuit dynamics. Decisions about simulation models are often framed in terms of “slow” and “fast” dynamics, though formal definitions of slow and fast will depend on the context. This paper presents two formalizations of “slow” and “fast”: in terms of a signal’s bandwidth and in terms of model order reduction through Singular Perturbation Theory (SPT). The challenges of time-domain simulation in the context of IBR dominated systems have been discussed recently. In [1], the authors study the applicability of specific techniques to the simulation and modeling of systems with IBRs, from the signal processing perspective. A recent review [9] discusses existing and novel methods to accelerate Electromagnetic Transient (EMT) simulations in systems with IBRs. Composite system models for the network circuits, generators, and inverters of different types are described in [10], [11].

Scope & Contributions: This paper seeks to clarify the semantics used to describe time-domain simulation models and their applications to system-wide simulations in the presence of IBRs given the need to develop novel simulation techniques that can capture IBR dynamics more accurately. While several efforts have focused on IBRs device-level simulation models [12]–[14], this paper focuses on system-wide simulation models with an increased presence of IBRs and examines the implications for stability analysis. The objective is not to provide specific formulation or simulation-domain guidance but rather to interpret the assumptions and modeling approaches implicitly embedded in widely used simulation techniques and tools. Particular emphasis is provided to reviewing *Simplifications* and *Transformations* inherent in various time-domain simulation methods and discussing the capabilities and limitations of these approaches. The contributions of the paper are as follows:

- Provide a review of power systems time-domain simulation modeling approaches with applications to IBRs.
- Present a systematic discussion of the origins and underlying assumptions of different power systems dynamic modeling techniques, including application examples.
- Survey modeling approaches and terminology used in the literature and the level maturity of their implementation in commercial and research applications.

The paper is structured as follows: Section II discusses the definition of power systems time-domain simulation methods and introduces the taxonomy of the simulation models covered in this paper to facilitate the overall discussion. Section III reviews common simplifications and transformation techniques used in time-domain simulations relevant to defining the scope of simulation model definitions. Section IV discusses relevant aspects of network and device modeling in the context of time-domain simulation methods with examples of how simplifications and transformations are used. In Section V, we discuss systems simulation focusing on definitions and

categorizations, and present an illustrative numerical test case. Finally, conclusions are presented in Section VI.

Notation: Lower-case letters x denote one-dimensional real variables, parameters, and functions; upper-case letters in the form F and $F()$ are used for matrices and functions respectively; arrows (as in \vec{x}) represent vectors of variables or parameters; $\langle \cdot \rangle$ denote phasors; and lower-case letters in the form \tilde{x} denote complex-valued variables, functions, or parameters. Finally, $j = \sqrt{-1}$.

II. TIME-DOMAIN SIMULATION

A time-domain simulation requires the specification of two “layers”: (1) a system model, including differential equations that describe the system’s physics and controls, and (2) a time stepping (or integration) algorithm. The choices made around the system model inform the integration algorithm requirements. This section defines what we mean by “simulation model” and provides a taxonomy of widely used methods.

A. Definition

A system simulation model is a set of dynamic equations in causal form for a collection of interconnected components expressed with explicit differential equations:

$$\frac{d\vec{x}(t)}{dt} = F(\vec{x}(t), \vec{y}(t), \vec{\eta}, t), \quad \vec{x}(t_0) = \vec{x}^0, \quad (1a)$$

$$\frac{d\vec{y}(t)}{dt} = G(\vec{x}(t), \vec{y}(t), \vec{\psi}, t), \quad \vec{y}(t_0) = \vec{y}^0, \quad (1b)$$

where $\vec{x}(t)$ and $F(\cdot)$ represent the devices (e.g., IBRs, machines, loads) states and equations with $\vec{\eta}$ parameters. The circuit dynamics of the network are represented as the subsystem $\vec{y}(t)$ and $G(\cdot)$ with network parameters $\vec{\psi}$.¹ The simulation model (1a)–(1b) can be used to represent real- and complex-valued signal analysis.

Given the system model (1a)–(1b), a simulation can be defined as follows: given an initial condition for the device and network states $\vec{x}(t_0), \vec{y}(t_0)$, advance the solution in time t from one point to the next considering a discrete timeline $\{t_0, t_1, \dots, t_n, \dots, T\}$. A simulation requires a stepping algorithm that finds the solution at time t_{n+1} given values of the involved variables over $\{t_0, t_1, \dots, t_n\}$.

In steady state, voltage and current state variables in the model defined by (1a)–(1b) are sinusoidally time-varying, making the dynamic response dependent on the value of t . Without some form of transformation, differential equations describing time-invariant system dynamics do not have well-defined equilibrium points. Solving time-varying nonlinear systems is expensive because integration algorithms use fixed time steps, and equilibrium points cannot be defined. Additionally, modeling three-wire three-phase power system components can result in intractable expressions with cross-coupling terms (for example, in the case of asymmetrical circuits or

¹Simulation models could include a spatial component, as in the case of circuit models that consider traveling waves. In cases where the behavior of traveling waves is relevant, time-delay equivalents such as the Bergeron model are commonly used and can be implemented via (1a)–(1b).

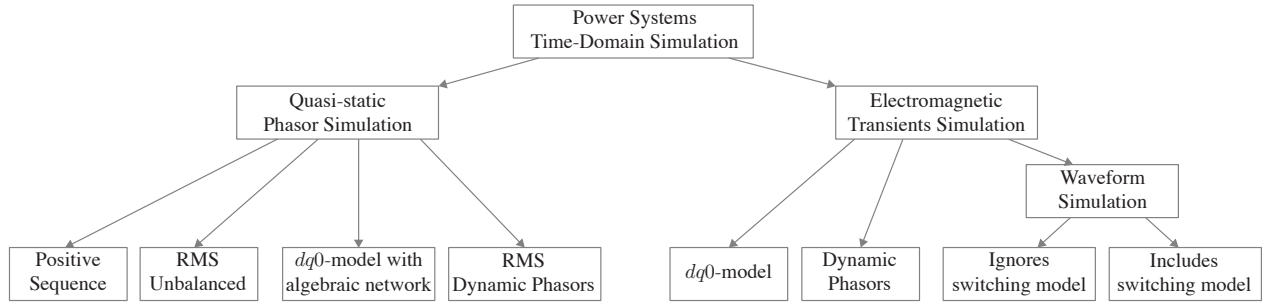


Fig. 2. Taxonomy of power systems time-domain simulation models.

unbalanced signals).² As we will see, *simplifications* and *transformations* influence the maximum required discretization step, Δt , and the number of states required to model the dynamics of interest.

B. Taxonomy

In power systems, time-domain simulation is roughly classified into two groups: 1) *Quasi-Static Phasor (QSP) Simulations* in which the transmission system circuits dynamics are represented algebraically as discrete changes between steady-state operating points, and 2) *EMT Simulations* which include sufficient detail to capture fast dynamic phenomena. QSPs are used for the study of low-frequency phenomena that ranges from inertial response to frequency regulation. On the other hand, EMT simulations are used in settings where one wishes to capture the impact of line dynamics, converter switching, machine fluxes, and/or lightning surges.

Figure 2 depicts a taxonomy of time-domain simulation models found in the literature and covered in this paper. Though we have organized model types as subcategories of QSP models and EMT models, one can see there is a variety of different types of models within each category. We have organized model types roughly by the fastest time scale phenomena they are intended to capture. As we will explain in this paper, though modeling faster time scale phenomena requires more modeling detail, there are other important differences between these models. Their mathematical formulations, the numerical algorithms available to numerically integrate them, and the assumptions required to interface machines and other energy-conversion interfaces across a network differ in important ways within the taxonomy. These differences can introduce fundamental changes in model properties and output, influence the complexity of initializing model runs, and dictate the maximum allowable time step (and therefore, the computing time and data generated).

For practitioners, the definition of a simulation model is intertwined with the software environment used. Each simulation category (QSPs or EMT) has highly specialized models, algorithms, and modeling practices that have been developed over many decades. As a result, choosing a simulation model and its methods is inextricably tied to the

software environment and its capabilities. Therefore, in order to clearly talk about the difference between models in the taxonomy, we will introduce two broad classes of modeling choices: *simplifications* and *transformations*. The following section systematically reviews the broad space of potential simplifications and transformations. Subsequently, we discuss specific simulation tools in the context of these simplifications and transformations. This enables us to begin to understand the entire range of assumptions that go into different simulation tools and to move beyond the simple distinction of whether or not they are designed to study electromagnetic transients.

III. SIMPLIFICATIONS AND TRANSFORMATIONS

By “simplification” and “transformations,” we mean mathematical manipulations of state variables that preserve the validity of some portion of a model’s characterization of system physics and control loops. Transformations can have multiple equivalent formulations, and several works have developed a comprehensive analysis of transformations [16], [17] and arrived at equivalent conclusions to the ones presented here. Different from transformation, simplifications are aimed to reducing model complexity at the cost of an approximation to the real system dynamics.

A. Simplification: Averaging Dynamics

Averaging methods focus on determining how the behavior of a complicated time-varying system can be approximated by a time-invariant system [18]. Averaging techniques are critical to reducing the computational cost of conducting simulations by reducing model bandwidth requirements, which, in turn, enables simulations to increase the maximum allowable time step Δt . It is important to note that several quantities from a physical system can be averaged in a simulation model. For instance, averaging the commutation dynamics of the power electronics modules that operate in tenths of kHz bandwidth using a static representation [15]. To this end, methods like Average-Value Modeling formalize the formulations that replace discontinuous switching with continuous models to accurately represent the converter’s average behavior within switching intervals. In [19], the authors provide a detailed review of converter switching averaging. This paper focuses on the averaging of slower dynamics with bandwidth well below the kHz range that still challenge system level simulations. Averaging fast dynamics not related to switching,

²The terminology adopted follows [15], which uses *balanced* in the context of signals and *symmetric* in the context of circuits.

the integration step of a power system model can go from 50ms to as large as one second for low-frequency dynamics [20]. Phasor representations of signals are regularly used as simplifications in power system simulations, and we discuss several approaches in the remainder of this subsection, along with their connection to averaging.

1) *Steady State Phasors*: Steady state phasors are commonly defined in engineering as it applies to signals $s(t) = s_{pp} \cos(\varrho t + \theta) = \sqrt{2} \operatorname{Re}\{S e^{j(\varrho t + \theta)}\}$, on which the “phasor” $S = \frac{s_{pp}}{\sqrt{2}} e^{j\theta}$ is expressed using the wave’s root-mean-square value instead of the instantaneous value. This definition requires stationary conditions and homogeneous frequency³

2) *Dynamic Phasors*: *Dynamic phasor* as a concept was introduced in the early 1990s, has received renewed attention as a mechanism for simulating systems including fast IBR dynamics. There are at least three independent but similar definitions of “dynamic phasor” in the literature, each developed using different approaches. The three approaches are motivated by the observation from averaging theory that the study of the signal envelope variations is sufficient to derive systems’ stability properties. Sanders *et al.* [21] introduced *dynamic phasors* via generalized averaging involving a time-dependent sliding-window interval $\mathcal{T}(t) = [t - T, t]$ for time-varying systems. In particular,⁴ consider the following expansion for a *nearly periodic* signal $s(t)$:

$$s(t) = \sum_{k=-\infty}^{\infty} \langle s \rangle_k(t) e^{jk\varrho t}. \quad (2)$$

The time-varying Fourier coefficients $\langle s \rangle_k(t)$, one for each harmonic component k , are recoverable as

$$\langle s \rangle_k(t) = \frac{1}{T} \int_{\tau \in \mathcal{T}(t)} s(\tau) e^{-jk\varrho \tau} d\tau, \quad (3)$$

and these are regarded as *dynamic phasors*. The time dependency of $\langle s \rangle_k(t)$ enables the formulation of a differential rule to capture continuous time behavior as follows:

$$\left\langle \frac{ds(t)}{dt} \right\rangle_k = \frac{d\langle s \rangle_k(t)}{dt} + jk\varrho \langle s \rangle_k(t). \quad (4)$$

extending dynamic phasors to complex periodic signals $s(t)$ is straightforward. For each $k\varrho$ where $\langle s \rangle_k(t) \neq 0$ there is a component at the negative frequency $-k\varrho$ with a phasor $\langle s \rangle_{-k}(t) = \langle s(t)^* \rangle_k^*$. We will refer to this approach to dynamic phasors as the *Fourier approach*. A variation of the *Fourier approach* described in this subsection is later employed in [22] to analyze machine fed load-commutated converters.

Another definition of dynamic phasors is derived from a communications-theoretic perspective [23]–[25]. Venkatasubramanian introduced *time-varying phasors* in [24] defining such a phasor via a linear operator $P()$, such that $P(s(t)) = \langle s \rangle(t)$. In other words, $P()$ maps a signal $s(t)$ a phasor. The definition of *time-varying phasors* begins with the idea that given a dynamic phasor of the form:

$$\langle s \rangle(t) = s_{pp}(t) e^{j\theta(t)}, \quad (5)$$

there exist a unique band-pass modulated signal

$$s(t) = \operatorname{Re} \{ \langle s \rangle(t) e^{j\varrho t} \} = s_{pp}(t) \cos(\varrho t + \theta(t)), \quad (6)$$

where s_{pp} is the signal’s amplitude. The operator $P()$ is defined for signals where it is possible to find a unique phasor $\langle s \rangle(t)$ such that $P^{-1}(P(s(t))) = s(t)$. The key property of $P()$ is that if the spectral content of $s(t)$ is slower than the carrier frequency ϱ , the operator maps to a unique phasor. Hence, the method is akin to a modulation operation to go from a time representation to a complex phasor representation.

From (6), it is possible to define the differential property of $P()$ as follows:

$$P\left(\frac{ds(t)}{dt}\right) = \frac{d\langle s \rangle(t)}{dt} + j\varrho \langle s \rangle(t). \quad (7)$$

The differential property in (7) is the same as the Fourier dynamic phasor in (4) for $k = 1$. We will refer to this approach to defining a dynamic phasor as the *linear operator approach*.

The third approach to deriving dynamic phasors is rooted in the Shifted Frequency Analysis (SFA) concept developed by Martí *et al.* [20], [26], and it is closely related to the definition of the linear operator $P()$ introduced in [24].⁵ SFA begins with the assumption that a power system dynamic signal is a band-pass, real-valued, and can be represented by a Fourier decomposition as follows:

$$s(t) = s_{pp,d}(t) \cos(\varrho t) - s_{pp,q}(t) \sin(\varrho t), \quad (8)$$

and the dynamic phasor is defined as $\langle s \rangle(t) = s_{pp,d}(t) + js_{pp,q}(t)$. It is composed of low-pass functions in quadrature $s_{pp,d}(t) = s_{pp}(t) \cos(\theta(t))$ and $s_{pp,q}(t) = s_{pp}(t) \sin(\theta(t))$. The procedure described by SFA provides a method to obtain $\langle s \rangle(t)$ through a *shifted frequency* representation of $s(t)$:

$$\langle s \rangle(t) = (s(t) + j\mathcal{H}\{s(t)\}) e^{-j\varrho t}, \quad (9)$$

where $\mathcal{H}()$ is the Hilbert transform [27]. Equation (9) shifts signal $s(t)$ with the form (8) by $-\varrho$. As a result, it centers all the signal’s dynamics around 0 Hz. The differential property for (9) can be derived from differentiating (9) resulting in (7). In each case, the definition of “phasor” corresponds to the complex envelope of a signal with a modulating frequency $k\varrho$ (with $k = 1$ only in the linear operator and SFA approaches, and arbitrary integer k in the Fourier approach). The three approaches reach the same operation for the differentiation of phasorial representation of a signal and its properties.

The definitions above provide several properties required to leverage dynamic phasors for time-domain simulation of average models. First, note that a dynamic phasor operation is interpreted as a band-pass modulation [20], [24] where a given time-varying signal $s(t)$ is demodulated into a set of dynamic phasors $\langle s \rangle_k(t)$ with a given carrier frequency ϱ . The implication is that the signal $s(t)$ needs to possess a well-defined Fourier transform, which requires that: 1) The integral of $s(t)$ needs to be well-defined over the period $\mathcal{T} = [t - T, t]$, i.e., (3) needs to be bounded, and 2) for a given frequency $k\varrho$, the signal $s(t)$ is narrow-band with a bandwidth $\mathcal{B} = [(k -$

³Refer to Section 1.4.1 [16] and its references for further details on the origins of the term “phasor”

⁴In this section ϱ represents signal frequency, ω_s denotes system frequency.

⁵In fact, Venkatasubramanian mentions that the time-varying phasor approach is inspired by the Hilbert transform, which is central to SFA.

1) ϱ , $(k+1)\varrho$] [28]. This demodulation perspective provides a definition of “slow” and “fast” dynamics of the system with respect to the modulating frequency ϱ and its harmonics as noted in [23]. In particular, the bandwidth (or speed) of the dynamic phasor is limited by the modulating signal frequency $k\varrho$ in order for the reverse transformation to be one-to-one. This discussion highlights that under certain conditions, it is possible to use an average model of the dynamics without any information loss.

Using dynamic phasors for simulation model averaging comes with potential trade-offs since the increase in the number of states can dilute the gains derived from using larger Δt [28]. This is particularly problematic in cases where the resulting average models are still time-varying. The practical implication of these limitations is that the dynamic phasor representation of a high-frequency (i.e., fast) signal could require many k components. It also implies that the representation of high-frequency dynamic behavior using a single carrier frequency may introduce error in the demodulation process [29].

3) *Representation of three-phase signals and models:* The definitions in Section III-A2 focus on “single-phase” complex signals. However, there is no unique application of dynamic phasors to poly-phase systems, contributing to the diversity of definitions and formulations when the technique is used for time-domain simulation. For instance, SFA and the linear operator are applied phase-by-phase to a three-phase abc in [20], [24], [30] to study unbalanced systems. In this case, each phase needs to comply with the requirements described in Section III-A2 to enable an exact representation of the underlying signals. Another implementation is used in [28], where the Fourier approach is used to develop models for each k^{th} harmonic required when modeling machines, FACTS, and HVDC-links. Similarly, the Fourier dynamic phasors were implemented in conjunction with sequence transformations in [31] to study unbalanced AC machines. The myriad implementations of dynamic phasors to three-phase signals and systems make it difficult to point out a universally accepted set of properties and limitations.

Transmission-level power systems analysis is generally concerned with modeling multi-phase system quantities with a common *system frequency* ω_s and an offset θ for each phase. For simplicity in the discussion that follows, we consider a three-wire three-phase signal $s_{abc}(t)$ (that satisfies $s_{abc}(t)^\top \mathbf{1} = 0$) of the form:

$$\vec{s}_{abc}(t) = \begin{bmatrix} s_a(t) \cos(\omega_s t + \theta_a(t)) \\ s_b(t) \cos(\omega_s t + \theta_b(t)) \\ s_c(t) \cos(\omega_s t + \theta_c(t)) \end{bmatrix}, \quad (10)$$

where $s_a(t)$, $s_b(t)$, and $s_c(t)$ are real-valued wave amplitudes, $\theta_a(t)$, $\theta_b(t)$, and $\theta_c(t)$ represent the phase difference between the waves, and the signal’s frequency is the *system frequency* ω_s , which is commonly assumed as a uniform “system frequency”. $s_{abc}(t)$ can be used to represent voltages, currents, electromagnetic flux or physical values like inductance.

In this paper, we approach the study of dynamic phasors for three-phase signals using a *space vector* representation that

provides a complex signal equivalent derived as follows:

$$\mathbf{s}(t) = c \begin{bmatrix} s_a(t) \left(e^{j(\omega_s t + \theta_a(t))} + e^{-j(\omega_s t + \theta_a(t))} \right) \\ s_b(t) \left(e^{j(\omega_s t + \theta_b(t))} + e^{-j(\omega_s t + \theta_b(t))} \right) \\ s_c(t) \left(e^{j(\omega_s t + \theta_c(t))} + e^{-j(\omega_s t + \theta_c(t))} \right) \end{bmatrix}^\top \begin{bmatrix} e^{j0} \\ e^{j\frac{2\pi}{3}} \\ e^{j\frac{-2\pi}{3}} \end{bmatrix}, \quad (11)$$

where the constant c is set to scale the vector’s magnitude. For an arbitrary three-phase signal, (11) permits representation in a two-dimensional vector as follows: [15], [17] (see Chapter 4 in [15] and [17]):

$$\mathbf{s}(t) = c \left(\mathbf{s}_+(t) e^{j\omega_s t} + \mathbf{s}_-(t) e^{-j\omega_s t} \right) \quad (12)$$

where the terms $\mathbf{s}_+(t)$ and $\mathbf{s}_-(t)$,

$$\begin{aligned} \mathbf{s}_+(t) &= s_a(t) e^{j\theta_a(t)} + s_b(t) e^{j(\theta_b(t) + \frac{2\pi}{3})} \\ &\quad + s_c(t) e^{j(\theta_c(t) - \frac{2\pi}{3})} \end{aligned} \quad (13)$$

$$\begin{aligned} \mathbf{s}_-(t) &= s_a(t) e^{-j\theta_a(t)} + s_b(t) e^{-j(\theta_b(t) - \frac{2\pi}{3})} \\ &\quad + s_c(t) e^{-j(\theta_c(t) + \frac{2\pi}{3})}, \end{aligned} \quad (14)$$

are complex-valued multipliers for the positive and negative frequency components, respectively. This shows that any three-phase signal without a zero-sequence component and with frequency ω_s can be modeled without loss of information using two complex-value dynamic phasors as long as $\mathbf{s}_+(t)$, $\mathbf{s}_-(t)$ comply with the requirements described in Section III-A2. This approach is used in [31] where the authors develop a model for signals of the form (12) for an unbalanced machine using (2)-(4) with $k = 1$ and $k = -1$ components.

The implication relevant to time-domain simulation is that it is not possible to directly model an arbitrary three-phase signal (10) with one complex phasor quantity—put formally: $\langle \mathbf{s}(t) \rangle \neq \langle \mathbf{s}(t) \rangle_+ + \langle \mathbf{s}(t) \rangle_-$. Nevertheless, if the signal is balanced—i.e., $s_a(t) = s_b(t) = s_c(t) = s(t)$ and $\theta_a(t) = \theta(t)$, $\theta_b(t) = \theta_a(t) - \frac{2\pi}{3}$, $\theta_c(t) = \theta_a(t) + \frac{2\pi}{3}$ —then components $\mathbf{s}_+(t)$, $\mathbf{s}_-(t)$ reduce to:

$$\mathbf{s}_+(t) = 3s(t) e^{j\theta(t)}, \quad \mathbf{s}_-(t) = 0, \quad (15)$$

which implies that $\langle \mathbf{s}(t) \rangle = \langle \mathbf{s}(t) \rangle_+$. The result in (15) showcases the effectiveness of averaging techniques in balanced systems: *the envelope of a balanced three-phase signal is completely determined by the positive-frequency phasor*. Handling unbalanced three-phase signals with dynamic phasors usually implies layering transformations as presented in [28], [30] where the authors employ unbalanced-three-phase to sequence components via the Fortescue transform [32] and finally get the dynamic phasors for the positive and negative components. However, even if a dynamic simulation requires modeling phasors for components at multiple frequencies, it can improve the solution times with respect to modeling directly in abc if the increase in Δt compensates for the increase in the number of states.

B. Reference Frame Transformations

The application of reference frame transformations in simulation models is ubiquitous since they are the basis of rotating electric machinery analysis and power electronic converter control. However, for developing simulation models, Park’s

Transform (or dq0 transform) [33] is the most commonly employed. Park's original use case was the transformation of the machine's rotor and the stator rotational mutual inductance to a time-invariant quantity. The applicability of the transform has been expanded to other devices and network quantities. Park's transform is defined as:

$$\vec{s}_{dq0}(t) = CT_p(\theta(t))\vec{s}_{abc}(t) \quad (16)$$

where $\theta(t)$ is the angle between the "reference axes" and the axes of rotation. The transform's matrix $T_p(\theta(t))$ can be defined arbitrarily for any $\theta(t)$, which leads to different formulations depending on the leading-lagging relationships between the d and q axis. This paper follows the convention in Standard IEEE-1110 [4], whereby the q-axis lags the d-axis and the a-phase is aligned with the d-axis to define the transformation matrix:

$$T_p(\theta(t)) = \begin{bmatrix} \cos \theta(t) & \cos(\theta(t) - \frac{2\pi}{3}) & \cos(\theta(t) + \frac{2\pi}{3}) \\ -\sin \theta(t) & -\sin(\theta(t) - \frac{2\pi}{3}) & -\sin(\theta(t) + \frac{2\pi}{3}) \\ 1 & 1 & 1 \end{bmatrix}. \quad (17)$$

While manipulations involving dynamic phasors hinge on assumptions concerning the frequency content involved in signals, the transform (16) can be applied to any three-phase signal (in both directions). Although the reference transform is valid and reversible for any combination of $\vec{s}_{abc}(t)$ and $\theta(t)$, transforming the system is *useful* for the purposes of simulation only with careful selection of $\theta(t)$. As discussed in [17], the choice for $\theta(t)$ can yield transformation matrices equal to the ones used in other transformations. For example, with $\theta(t) = \theta_0$, the $\alpha\beta 0$ /Clarke transformation is obtained. These transformations are widely applied in control design for converters or torque control for induction motors but are less useful for simulation model formulation applications.

In simulation models, the calculation of the angle $\theta(t)$ is usually done by integrating the frequency of the signal (10):

$$\theta(t) = \int_{t_0}^t (\omega_s + \Delta\omega_s(\tau)) d\tau + \theta^0. \quad (18)$$

where, respectively, ω_s and $\Delta\omega_s(t)$ are the frequency and its time-dependent variation. In a balanced system, the effectiveness of the transformation relies on using a reference frame with a constant frequency, i.e., $\Delta\omega_s(t) = 0$, such that we can obtain:

$$\vec{s}_{dq0}(t) = cT_p(\theta(t))\vec{s}_{abc}(t) \triangleq \vec{s}_+(t) \quad (19)$$

Under balanced conditions, Park's transform maps the three-phase signal's dynamic phasor $\vec{s}_+(t)$. The transformation reduces the simulation models by transforming the variables of the components to a rotating reference frame [34] which requires fewer variables without loss of information.

In interconnected device simulations, we can define the reference frame to reference transformation:

$$T_p(\theta_1(t))T_p(\theta_2(t))^{-1} = \begin{bmatrix} \cos \Delta\theta(t) & \sin \Delta\theta(t) & 0 \\ -\sin \Delta\theta(t) & \cos \Delta\theta(t) & 0 \\ 0 & 0 & 1 \end{bmatrix} \quad (20)$$

where $\Delta\theta(t) = \theta_1(t) - \theta_2(t) = \int_{t_0}^t (\Delta\omega_1(\tau) - \Delta\omega_2(\tau)) d\tau + \Delta\theta^0$. The above property implies that only the local reference

frames' frequency deviations are required for the system simulation. Moreover, the selection of common system frequency ω_s is of no consequence to the simulation results as long as there is a local $\Delta\omega(t)$ variable at the device model.

In the case of machine models, it is possible to define the change of the local reference frame frequency in terms of the rotor speed changes, i.e., $\Delta\omega(t) = \Delta\omega_r(t)$. This property was identified in [29], where the authors recognized that the machine rotor is a *perfect demodulator of the network signals*. This implies that each synchronous machine imposes, through its rotor angular speed, the frequency at the bus. Further, the "system frequency" is not a modeled quantity, nor is it required to represent the system dynamics accurately.

However, unlike electrical machine models, an IBR does not necessarily have a local reference frame. Hence, when simulating IBRs, the relationship of the device model with ω_s is dictated by the controls and their representation. For instance, many IBR control structures rely on frequency measurements at the local bus for the internal controls, introducing a heretofore unproblematic requirement in system simulations: namely, reliably modeling frequency dynamics at the bus. When modeling control schemes that require frequency measurements, the idealized frequency measurement is modeled as follows:

$$\Delta\omega_{\text{bus}}(t) = \frac{d}{dt} \tan^{-1} \frac{V_{q,\text{bus}}(t)}{V_{d,\text{bus}}(t)}. \quad (21)$$

The implication of having to estimate the local frequency in a simulation is that (21) relies on the value of the voltage states to estimate the local bus frequency. As a result, the frequency deviations' impact on the simulation becomes dependent on the network model's assumptions. Further, modeling frequency measurement with (21) suggests that simplifications in the network dynamics can mischaracterize the effects of frequency deviations on the controls and introduce further deviations from the real-world behavior of the IBR.

Recent works have looked at the theoretical underpinnings of the system's modeling and the definition of system frequency in simulation models to develop novel theories about the relationships between energy and system frequency [16], [35] to develop a rigorous perspective that considers the inclusion of IBRs. However, this is still an area under active development, and there are not widely adopted practices to manage the frequency selection for large-scale simulations.

C. Singular perturbation theory (SPT)

In the power systems literature, it is common to make approximations that reduce the number of states modeled [36]. The justifications for several reductions are based on practical knowledge; however, these approximations have also been formalized in terms of time-scale separation arguments derived from SPT of system dynamics [37], [38].⁶ In the context of the model (1a)–(1b), SPT identifies two state categories: "slow" states (\vec{x}_s , \vec{y}_s) and "fast" states (\vec{x}_f , \vec{y}_f). Fast states are multiplied by a small positive real scalar ε that represents

⁶The reader is referred to [38] for the foundations of SPT.

all the small parameters to be neglected. The dynamics are then presented as:

$$\dot{\vec{x}}_s = F_s(\vec{x}, \vec{y}, \vec{\eta}, \varepsilon), \quad \dot{\vec{y}}_s = G_s(\vec{x}, \vec{y}, \vec{\psi}, \varepsilon) \quad (22)$$

$$\varepsilon \dot{\vec{x}}_f = F_f(\vec{x}, \vec{y}, \vec{\eta}, \varepsilon), \quad \varepsilon \dot{\vec{y}}_f = G_f(\vec{x}, \vec{y}, \vec{\psi}, \varepsilon) \quad (23)$$

SPT involves finding the trajectories of a dynamical system as $\varepsilon \rightarrow 0$. If the conditions are met, it is possible to set $\varepsilon = 0$ and reduce (23) to algebraic equations. The requirement to perform a reduction in the number of dynamic states, is that the algebraic equations (23) in the domain of interest have distinct roots (i.e., the model is in *standard form* [38]):

$$\vec{x}_f = R_x(\vec{x}_s, \vec{y}_s, \vec{\eta}), \quad \vec{y}_f = R_y(\vec{x}_s, \vec{y}_s, \vec{\psi}). \quad (24)$$

If the roots of (24) are distinct, it is possible to guarantee, via eigenvalue analysis, that during a transient the fast dynamics will not diverge. As described in [38], most of this analysis is done on the “boundary layer system” that imposes requirements on the eigenvalues of the Jacobian of F_f and G_f . Distinct isolated roots enable the use of variable substitution which results in a well-defined reduced model at a specific root value as follows:

$$\dot{\vec{x}}_s = F_s(\vec{x}_s, \vec{y}_s, R_x(\vec{x}_s, \vec{y}_s, \vec{\eta}), \vec{\eta}), \quad (25a)$$

$$\dot{\vec{y}}_s = G_s(\vec{x}_s, \vec{y}_s, R_y(\vec{x}_s, \vec{y}_s, \vec{\psi}), \vec{\psi}). \quad (25b)$$

System (25a)-(25b) is the *quasi-steady-state model*. These definitions based on SPT provide a different definition of “slow” and “fast” in a simulation, this time, in terms of the “speed” of some states with respect to others. SPT provides conditions under which the fast states may rapidly converge to a root that approaches the final value of the state, i.e., $\vec{x}_f \rightarrow R_x(\vec{x}_s, \vec{y}_s, \vec{\eta})$ and $\vec{y}_f \rightarrow R_y(\vec{x}_s, \vec{y}_s, \vec{\psi})$.

The theoretical underpinnings of SPT justify the practice of neglecting line capacitance and the resulting voltage dynamics in short-length lines due to the small value of the current drawn from the shunt impedance. SPT is used in [39], [40] to show that modeling current flows over the network via the admittance matrix \mathbf{Y} is a reasonable approximation of the integral manifold. Such approximations have also been shown to be valid for small signal analysis and are typically used for studying intra- and inter-area electromechanical oscillations, as well as stabilizer parameter tuning [40].

IV. NETWORK AND DEVICE MODELING

The device and network models’ level of detail determines the requirements placed on time-domain simulation solution methods. The simulation models must accurately capture the interactions across the different timescales. Thus, both network and device dynamic models formulations must be consistent in their assumptions.

A. Network modeling

As discussed in Section II-B, the representation of network circuit dynamics in the simulation models is a major distinguishing attribute in establishing the taxonomy. The transmission line model formulation has significant importance on the time-domain simulation category selection since it

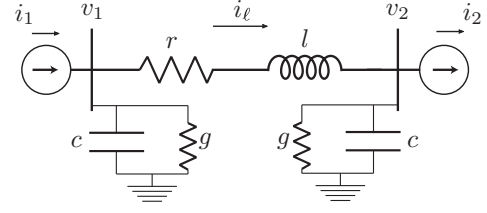


Fig. 3. One-line diagram of a connection between two three-phase sources.

impacts the bandwidth [34] and time-constant of the states [7] added to the model.

The detailed dynamic model of a transmission line is a model using Partial Differential Equations (PDEs) for the voltage and current across the line length with distributed parameters. However, it is difficult to include this level of detail in time-domain simulation tools, and experience shows that the impacts of using simplified models are not significant for most applications. The appropriateness of using simplifying assumptions depends on the line length: *long* (> 200 km), *medium* (80-200 km), and *short* (< 80 km) [40]. In *short* lines, shunt elements are not considered ($C' = G' = 0$), reducing the model to a series r - l circuit [40]. Another common simplification is the lossless line assumption ($R' = G' = 0$), which results in a simplified two-port model interfaced via a current source with time delay $\tau = d\sqrt{L'/C'}$ (where d is the line length) [41]. The Bergeron line model extends the delayed current-source model approximating the series resistance losses by adding lumped resistances at both ends of the two-port system.

The lumped parameter π -circuit of a transmission line results from a quasi-static analysis when voltage and currents are assumed to be sinusoidal functions with constant frequency. The use of Ordinary Differential Equations (ODEs) of the RLC π -model is a *simplification* of the PDEs, and the accuracy of this approach depends on the line parameters and specific phenomena studied [40]. The following example showcases the transformation for the π line model and the application of simplifications.

Example 1: Consider the three-phase lumped-circuit elements π -line model in Fig. 3. The per-unit voltage and line dynamics of a symmetrical circuit are captured by ODEs:

$$\frac{l}{\Omega_b} \frac{d}{dt} \vec{i}_{abc,\ell}(t) = [\vec{v}_{abc,2}(t) - \vec{v}_{abc,1}(t)] - r \vec{i}_{abc,\ell}(t), \quad (26a)$$

$$\frac{c}{\Omega_b} \frac{d}{dt} \vec{v}_{abc,1}(t) = [\vec{i}_{abc,1}(t) - \vec{i}_{abc,\ell}(t)] - g \vec{v}_{abc,1}(t), \quad (26b)$$

$$\frac{c}{\Omega_b} \frac{d}{dt} \vec{v}_{abc,2}(t) = [\vec{i}_{abc,\ell}(t) - \vec{i}_{abc,2}(t)] - g \vec{v}_{abc,2}(t), \quad (26c)$$

in which Ω_b is the base frequency in rad/s. The value of Ω_b depends on the specific system under study, it can take the values $2\pi 60$ or $2\pi 50$ rad/s. $\vec{i}_{abc,1}(t)$ and $\vec{i}_{abc,2}(t)$ are three-phase real-valued quantities related to adjoining dynamical systems. The dynamic π -model model (26) has nine states, and it is commonly used on waveform simulations (see Fig. 2) and as the base to develop transformed line models.

The system of equations (26a)-(26c) can be transformed using Park’s transformation (16) with a fixed frequency ω_s to

yield the following dynamics in the dq reference frame:

$$\frac{l}{\Omega_b} \frac{d}{dt} \mathbf{i}_\ell(t) = [\mathbf{v}_1(t) - \mathbf{v}_2(t)] - (r + j\omega_s l) \mathbf{i}_\ell(t), \quad (27a)$$

$$\frac{c}{\Omega_b} \frac{d}{dt} \mathbf{v}_1(t) = [\mathbf{i}_1(t) - \mathbf{i}_\ell(t)] - (g + j\omega_s c) \mathbf{v}_1(t), \quad (27b)$$

$$\frac{c}{\Omega_b} \frac{d}{dt} \mathbf{v}_2(t) = [\mathbf{i}_\ell(t) - \mathbf{i}_2(t)] - (g + j\omega_s c) \mathbf{v}_2(t), \quad (27c)$$

where $\mathbf{v}(t) = v_d(t) + jv_q(t)$, $\mathbf{i}(t) = i_d(t) + ji_q(t)$, $\mathbf{i}_1(t)$, $\mathbf{i}_2(t)$, and $\mathbf{i}_\ell(t)$ are the transformed $\vec{i}_{abc,1}(t)$, $\vec{i}_{abc,2}(t)$, $\vec{i}_{abc,\ell}(t)$ output currents. If the signals $\vec{i}_{abc,1}(t)$ and $\vec{i}_{abc,2}(t)$ are balanced, the resulting model eliminates any sinusoidal time-varying characteristic and reduces the model to six time-invariant differential equations. Under balanced conditions, (27a)–(27c) are, together, the dynamic phasor representation of the network quantities, reflecting the common approach to capturing line dynamics in time-domain simulations as presented in Fig. 2. If $\vec{i}_{abc,1}(t)$ or $\vec{i}_{abc,2}(t)$ is unbalanced or contains harmonics, the dq transformation yields time-varying signals, and the benefits could be minimal with respect to abc modeling as in (26a)–(26c). The results of this transformation do not generalize to arbitrary unbalanced three-phase signals. For unbalanced signals, it is required to follow the approach in [30] where the authors first obtain balanced equivalents for each positive and negative sequence components and afterwards introduce the dq0 transform.

The transformed ODE system (27a)–(27c) can be further simplified employing SPT since the terms ℓ/Ω_b , $c/\Omega_b \approx 10^{-3}$ have small values in most systems operating at 50 or 60 Hz. Making the left-hand-side of (27a)–(27c) zero yields the following algebraic map:

$$\begin{bmatrix} \mathbf{i}_1 \\ -\mathbf{i}_2 \end{bmatrix} = \begin{bmatrix} \mathbf{y}_\ell + \mathbf{y}_c & -\mathbf{y}_\ell \\ -\mathbf{y}_\ell & \mathbf{y}_\ell + \mathbf{y}_c \end{bmatrix} \begin{bmatrix} \mathbf{v}_1 \\ \mathbf{v}_2 \end{bmatrix}, \quad (28)$$

where $\mathbf{y}_l = (r + j\omega_s l)^{-1}$ and $\mathbf{y}_c = g + j\omega_s c$. This model formulation is equivalent to commonly used current-injection representation of the network model $G(\cdot)$ [24], [25], [34]:

$$\frac{d\vec{\mathbf{x}}(t)}{dt} = F(\vec{\mathbf{x}}(t), \vec{\mathbf{v}}(t)), \quad (29a)$$

$$0 = I(\vec{\mathbf{x}}(t), \vec{\mathbf{v}}(t)) - \mathbf{Y}\vec{\mathbf{v}}(t). \quad (29b)$$

If the devices' model $F(\vec{\mathbf{x}}(t), \vec{\mathbf{v}}(t))$ only accounts for low-frequency neglecting high-frequency dynamics like stator fluxes or fast controls, the use of simplifications and transformations turns the time-variant dynamic model (1a)–(1b) to an index-1 Differential Algebraic Equation (DAE)⁷ Note that this formulation coincides with the single-phase steady-state phasor representation commonly used for QSP (or “positive sequence”) simulations; we will provide details on this taxonomy in Section V.

The accuracy of the reduced order model depends on the term that multiplies the derivative (ℓ/Ω_b and c/Ω_b in (27a)–(27c)) and its proximity to zero. This approximation error is typically observed in the system's dynamic response over a

⁷Index is a notion used in the theory of DAEs for measuring the distance from a DAE to its equivalent representation as an ODE. Index-1 DAEs can be solved in principle by substituting the values of the algebraic variable in the differential equations [42].

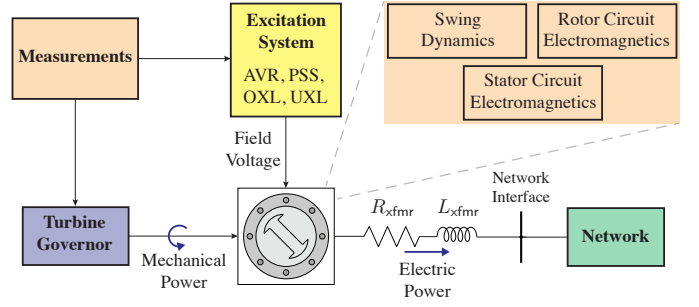


Fig. 4. Simplified synchronous generator block diagram.

disturbance near time zero [39]. If $\varrho = \omega_s$, this representation yields a quasi-static model of the network (also known as *time-varying phasor*) representation of the network [24], [25], [43].

The model representation in (29a)–(29b) has been justified in practice since it improves computational performance in large system transient stability studies without a significant loss of accuracy [29], [36]. The relative error introduced by (29b) is proportional to the ratio of the variation with respect to the carrier frequency. For instance, rotor dynamics in the range of 2 Hz introduce an error of around 3%. As a result, simulation tools use models that ignore the dynamics of the electrical network and should not be used to investigate phenomena such as sub-synchronous resonance, control interactions, and oscillations or phenomena with dynamics > 10 Hz [29].

B. Synchronous Generator Modeling

A typical disaggregation of a simulation model for a synchronous generator depicting mechanical, electrical, and electromagnetic dynamics is shown in Fig. 4. The abc three-phase model of a synchronous generator includes time-varying inductance terms due to the rotation of the rotor's electromagnetic field. The application of Park's transform significantly reduces model complexity by eliminating time-varying terms [33], [40]. The resulting machine model is composed of stator and rotor voltage equations, rotor flux linkage equations, and the rotor swing dynamics [40].

Example 2: Although it is possible to perform simplifications in any portion of the generator model, machine models are the prime candidate for reducing the simulation model's complexity. Take the stator voltage equations in dq assuming a balanced system and $\omega_r \approx 1$:

$$\frac{1}{\Omega_b} \frac{d}{dt} \psi_{dq} = e_{dq} + r_a i_{dq} - j\psi_{dq}. \quad (30)$$

In a machine model, the base frequency term $\Omega_b^{-1} \approx 10^{-3}$ is relatively small in systems operating at 50 or 60 Hz. Hence, employing SPT, it is possible to set the term $\Omega_b^{-1} \dot{\psi}_{dq} = 0$ and reduce the flux dynamics (30). The simplification implies that the terms ψ_{dq} decay very rapidly after a perturbation, as observed in practice. This simplification also removes high-frequency transients and fundamental frequency components in the currents i_d and i_q , which in turn also reduces the bandwidth of the model allowing larger time steps in the simulation execution. Once high-frequency terms are eliminated it is possible to include other approximations to reduce model

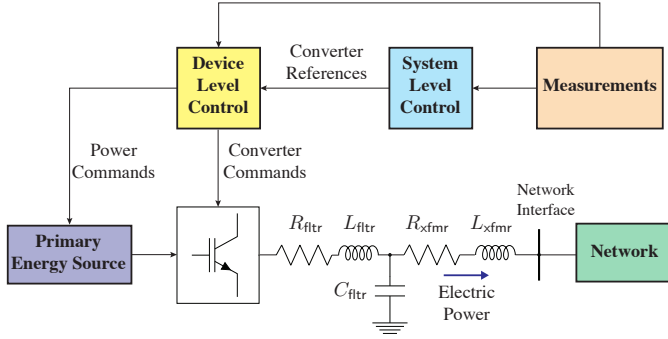


Fig. 5. Simplified converter block diagram.

complexity. For instance, the simplifying assumption that the per-unit value of ω_r is a fixed value 1.0 in equations (30). This simplification can be taken one step further via variable substitution of ψ_{dq} in the computation of the air-gap torque directly using voltages and currents as follows:

$$\begin{aligned}\tau_e &= \psi_d i_q - \psi_q i_d = (e_q + r_a i_q) i_q - (-e_d - r_a i_d) i_d \\ &= e_d i_d + e_q i_q + r_a (i_d^2 + i_q^2)\end{aligned}\quad (31)$$

The resulting model has the property of representing the energy balance at the shaft of the machine in terms of a QSP representation of the power at the stator.

C. Inverter Based Resources (IBR) Modeling

Energy conversion is fundamentally different in IBRs compared to synchronous generators. Instead of using a rotational magnetic field, IBRs synthesize voltages through high-frequency switching, introducing high-frequency dynamics into the synthesized voltages and realized currents. Despite the high-frequency behavior, IBRs include output filters and controllers with low-pass filters tuned to regulate average values; these aspects readily provide the rationale to disregard switching-level dynamics from IBR models intended for system-level studies [15].

IBR simulation models are structured according to the cascaded control architectures used in the field (see Fig. 5). IBR controls employ transformations to reduce the number of control loops and produce and regulate three-phase signals (of the form (10)); in this setting, transformations facilitate avoiding the regulation of sinusoidal signals, which requires high-order controls [15]. IBRs controls commonly employ Park's Transform since it has the property of reducing the controls' bandwidth requirements in order to achieve zero steady-state error. Hence, the model developer needs to be more aware of the effects that simplifications could have, not just on the model precision but also on the reliability of the control performance [11].

Models used to represent IBR dynamic behavior can either be Original Equipment Manufacturer (OEM) specific or generic [44], [45]. The wide variety of control architectures and topologies poses a challenge in the development of simulation models for IBRs. The level of detail used to model each sub-component depends on the study requirements, and—as in the case of generators—there needs to be consistency between

the device timescales and the remainder of the system model. For instance, in EMT IBR models, the dynamic behavior of the filter is commonly represented in detail, given that, in EMT simulation, the dynamics of the lines are also included. On the other hand, in QSP models, IBR “fast” controls may not be included if the rest of the system model's time constants are significantly larger than the controller's time constants. The fact that IBRs model dynamics can extend over multiple timescales depending on the control architecture and the time constants makes it challenging to determine whether a particular control can be reduced or should be modeled in detail. For this reason, the performance of a model needs to be verified against equipment behavior before integration into existing software tools. A contemporary example of such a transition is the IBR model for low short circuit systems [46] which has now been named as the REGC_C model under the generic suite of models for IBRs. Note that the intent of this paper is not to indicate that OEM or generic models belong to a specific category of simulation; both models can be implemented for quasi-static or EMT simulations. Rather, the intent is to assert that device models need to match the overall system assumptions.

Example 3: One of the possible simplifications for converter models in power system studies relates to local voltage and current controllers. As described in [5], [47], the internal controller involves two cascading PI controllers:

$$k_{iv}^{-1} \frac{d}{dt} \phi = -k_{pv}^{-1} \phi + k_{pv}^{-1} k_{iv}^{-1} (i_{cv}^{\text{ref}} - j C_{ftr} v_o), \quad (32a)$$

$$k_{ic}^{-1} \frac{d}{dt} \gamma = -k_{pc}^{-1} \phi + k_{pc}^{-1} k_{ic}^{-1} (v_{cv}^{\text{ref}} - j L_{ftr} i_{cv}), \quad (32b)$$

where ϕ are the integrator states (for d and q axes) of the voltage controller, intended to track the capacitor voltage v_o to a reference provided from the system level control v_o^{ref} , while γ are the integrator states of the current controller, intended to track the converter current output i_{cv} to a reference provided from the voltage controller i_{cv}^{ref} . The output of these controllers will output the converter voltage command v_{cv}^{ref} . Similar to Example 1, simplifications of the device level controllers dynamics can be argued from SPT since the integral gains k_{iv}^{-1}, k_{ic}^{-1} can be significantly small due to timescale separation requirements [47], [48]. In practice, this simplification of inner controls is equivalent to assuming that system-level control references are tracked without error.

Eliminating the internal current controls can also be extended to the filter dynamics in certain settings [48]. Since the filters are RLC circuits designed to attenuate high-frequency switching phenomena, they usually exhibit time constants around 10^{-3} s and can be eliminated using the same procedure as in Section IV-A. The resulting simplified model is a controlled voltage source behind a transformer impedance, where the voltage values are determined by the system-level control dynamics.

V. SIMULATION CATEGORIES

Table I summarizes common simulation categories and associated characteristics based on the taxonomy in Fig. 2. The model properties are split between the larger categories

TABLE I
SIMULATION CATEGORY REVIEW AND CLASSIFICATION

| Simulation Category | Name | Multiple Frequencies / Asymmetrical / Unbalanced | Network Representation | Software Availability |
|---|---|--|------------------------|-----------------------|
| Quasi-static phasor Simulation | <ul style="list-style-type: none"> • Positive Sequence • RMS Balanced • Electromechanical[†] • Transient Stability[†] | No | Single Phase | Mature |
| | • RMS Unbalanced | No* | Symmetrical Components | Mature |
| | • dq0-model with algebraic network | Yes | dq0 | Research |
| | • RMS Dynamic Phasor | Yes | <i>abc</i> or dq0 | Research |
| Electromagnetic Transients (EMT) Simulation | <ul style="list-style-type: none"> • Waveform • Point-on-Wave • <i>abc</i>-model | Yes | <i>abc</i> | Mature |
| | • dq0-model | Yes | dq0 | Research |
| | • Fast Time-Varying Phasor | Yes | <i>abc</i> or dq0 | Research |
| | • Dynamic Phasor | Yes | <i>abc</i> or dq0 | Research |

[†]These are commonly used for balanced systems, but they can be formulated for unbalanced networks as RMS Unbalanced model.

*The unbalanced network is handled algebraically by connecting the symmetrical circuits into a single phase.

of QSP and Electromagnetic Transients (EMT) given the commonalities in modeling assumptions. The main difference between the two categories stems from the representation of the network circuits. We have identified the modeling of the network circuits as the main determinant of a simulation model's numerical properties, available solution techniques and resulting computational requirements.

A. QSP

QSP models are narrow-band simulation models that focus on dynamics that do not deviate significantly from the steady-state frequency. In most software implementations, the integration method independently solves the device and network equations using an algebraic representation of (1b).

1) *Positive Sequence*: Also called *Root Mean Square (RMS) balanced* simulation; this is a QSP simulation where the balanced network is modeled using a single phase, the positive sequence. These models are formulated in the form of DAEs of the general form (29a)-(29b) and use solution strategies derived from the Partitioned-Explicit solution methods, relying on the assumption that the differential portion of the DAE is not stiff. These types of simulators are primarily designed for the analysis of machine angles in balanced transmission systems. This simulation category is also commonly called *Electromechanical* or *Transient Stability* simulations.

2) *RMS Unbalanced*: This is a simulation used to analyze non-symmetrical network circuits. The network is modeled using symmetrical components while keeping the representation algebraic. In this simulation, the dynamic components feed into the positive sequence subset of equations, and the three sequence networks are simplified using circuit algebra depending on the type of fault [24]. These models are commonly used to evaluate the system's transient behavior during and after unbalanced faults.

3) *RMS Dynamic Phasors*: This approach is based on constructing the model using Fourier Dynamic Phasor as defined in Section III-A2. This approach employs the same right-hand-side from (27a)-(27c) to model the network circuit. However, the derivative terms (left-hand side) are neglected since, in most RMS models, they represent faster dynamics

than the devices' models. This model produces a subset of equations (29a)-(29b) for each k^{th} harmonic component that can be integrated as a system of DAEs. The model's accuracy depends on the number of harmonics considered in the model and whether the dynamics around each harmonic possess the required properties to neglect the left-hand side derivative [28].

4) *dq0-model with algebraic network*: This type of simulation model is obtained by performing a dq0 transformation and assuming a steady state (e.g., by setting the left-hand side of (27a)-(27c) to zero). In the balanced case, this model is equivalent to *positive sequence*. When modeling an asymmetric network and/or harmonics, the method can increase the minimum Δt , but its usefulness is limited since it results in a time-varying model.

QSP simulation software tools are highly developed for system-level balanced analysis within the positive sequence category. For instance, PTI PSS/E, GE PSLF, PowerTech Lab's TSAT, and PowerWorld, among others, are some of the tools that share common solution methods and models. The model libraries are generic and developed in coordination with Independent System Operators (ISOs) standards and practices.

B. Electromagnetic Transients

EMT models are simulation models that can consider a diverse range of dynamic phenomena and are commonly implemented in studies that can significantly deviate from steady-state frequency. These are usually employed to study high-frequency phenomena, such as overvoltages, harmonic propagation, sub-synchronous resonance, and transient recovery voltages, among others [49]. Within this category, there is a large variety of modeling and computational approaches depending on the techniques used to limit the computational cost of executing the simulations.

1) *Waveform simulation*: A waveform simulation, also known as *point-on-wave* simulation or *abc*-simulation, is the most comprehensive implementation of EMT simulations. These simulation models represent the full wave throughout the entire simulation, which results in a time-variant model. As a result, these models require special consideration when initializing the simulation and choosing integration techniques.

To capture fast electromagnetic phenomena, these simulations usually feature more detailed transmission line models than the π -model (as described in Section IV-A). A waveform simulation allows the use of distributed models such as the Bergeron or frequency-dependent models. A waveform simulation can include detailed converter switching dynamics; it uses similar methods but employs piece-wise continuous models between switching instants and requires additional equations and solution methods to capture converter transistors' ON/OFF switching behavior.

2) *dq0-model*: A dq0-model is used to model the network in a rotating reference frame commonly modeled using the *transformed* π -model from (27a)-(27c). In the balanced case, also known as a *fast time-varying phasor* simulation [25], the model results in a time-invariant formulation that yields the same initialization routine of the positive-sequence model, but the simulation can represent the network dynamics limited only by the π model assumptions. Since the network is now modeled using only ODEs (i.e., there are no longer algebraic equations in the network model), the system model becomes a series of stiff ODEs because of the multi-rate nature of the system dynamics. As a result of the increased stiffness, finding the solution to the model might require the use of Simultaneous-Implicit solution methods [36]. Most of the benefits of this formulation are lost when used in unbalanced networks or with harmonics since the model results in time-varying signals that have similar requirements to *waveform simulations*.

3) *Dynamic Phasors*: This approach requires constructing that the model be formulated using Dynamic Phasors (see Section III-A2). Dynamic phasors are useful when the frequency spectrum of power system transients are multiple narrow-banded signals centered around multiple harmonics of a fundamental frequency ϱ . The choice of ϱ depends on the application; when employed to model converters, it could be the switching frequency, or in the case of system-level analysis, ω_s is a common choice. This approach can be implemented in several ways depending on the application, and if done correctly, the resulting model will be time-invariant but at the expense of additional states. A time-variant model enables other analytical techniques, such as sensitivity studies via small-signal analysis at equilibrium points making the approach practical beyond the formulation of simulation models. As shown in [28], dynamic phasors are helpful if the computational efficiency gained by reducing the model's bandwidth (and usage of adaptive time stepping techniques) outweighs the cost of increasing the number of states.

The most developed software solutions for EMT simulations focus on waveform dynamics with and without converter switching and include models for very detailed component-level analysis. Examples of software environments are PSCAD, EMTP®, Simulink, PLECS, among others.

C. Numerical integration methods considerations

In power systems applications, it is common to use numerical integration methods that, in part rely on the use of transformations and simplifications—thus embedding model-

ing assumptions into most simulation applications. In this subsection, we highlight important factors related to the numerical integration of simulation models as they relate to the model's formulation. See Chapter 2 in [50] for an in-depth look at choosing numerical integration methods for continuous-time simulation.

The literature on numerical integration methods applied to specific simulation categories is extensive. QSP simulations based on the index-1 DAE model (29a)–(29b) can use the “Partitioned-Solution method” which solves the differential equations separately from the algebraic equations, or a “Simultaneous-Solution method” which jointly solves both differential and algebraic equations. In [36], B. Stott presents a detailed account of the solution techniques applicable to QSP simulations and a historical account of why the field mostly converged to the use of partitioned methods. Waveform EMT simulations mostly employ the numerical integration substitution technique with a trapezoidal rule for integration as originally developed by Dommel [41] to simulate circuit behavior. In [51], the authors cover in detail the evolution of the “Dommel Method” and how to address limitations like the modeling of nonlinear elements and switching.

Regardless of the simulation category, the model choices have impacts on the integration techniques. This is particularly critical when considering trade-offs between accuracy and solution speed.

1) *Step size and integration approximation error*: Consider the Taylor approximation of a trajectory for a model defined by (1a)-(1b) as follows (we simplified the notation by collecting the arguments of the function F and G):

$$\vec{x}(t + \Delta t) = \vec{x}(t) + F(\cdot, t)\Delta t + \frac{dF(\cdot, t)}{dt} \frac{\Delta t^2}{2!} + \dots \quad (33a)$$

$$\vec{y}(t + \Delta t) = \vec{y}(t) + G(\cdot, t)\Delta t + \frac{dG(\cdot, t)}{dt} \frac{\Delta t^2}{2!} + \dots \quad (33b)$$

The approximation accuracy and computational cost of a numerical integration method depend on the step size, Δt , and the integration method order. Reducing Δt can improve accuracy by reducing the relative importance of high-order terms, but it comes at the expense of more algorithm iterations. On the other hand, higher-order approximations tend to be more accurate and allow for a larger Δt but require the evaluation of more terms. As discussed in [50], if the largest error tolerated within a single iteration is 10^{-n} , it is best to choose at least a n^{th} order algorithm. One of the main motivations for using simplifications and transformation in simulation models is to enable larger Δt without compromising the accuracy of the modeled states. For example, reference-frame transformations and dynamic phasors allow the modeling of fast time-varying states using envelopes. This, in turn, permits larger time steps than those required by full waveform models. Further, if the model complies with the requirements to employ SPT, the differential terms that represent fast dynamics (e.g., (32a)-(32b)) can be eliminated, further increasing the required minimum Δt required for a given accuracy, and accelerating computation.

Although simulation accuracy depends on the order and time step-length, most commercial software tools do not

provide a mechanism to adjust the integrator order. As a result, time step reduction is the only option to adjust the simulation time and accuracy.

2) *Model stiffness considerations*: Although there is no widely accepted definition of model stiffness, a classical measure is the stiffness ratio, σ , defined as:

$$\sigma = \frac{\text{Re}(\lambda_{\max})}{\text{Re}(\lambda_{\min})}(\Delta t), \quad (34)$$

where $\text{Re}(\lambda_{\max})$ and $\text{Re}(\lambda_{\min})$ are the real parts of the largest and smallest eigenvalues, respectively. The challenges of simulating systems with IBRs stem from interactions across time scales, and the requirements to include fast electromagnetic dynamics increases model stiffness [7]. Explicit integration methods, like Adams-Bashforth, widely used in QSP simulation software [52], have difficulty coping with highly stiff simulation models that result from the simultaneous modeling of electromechanical and electromagnetic phenomena.

Implicit numerical integration methods can overcome explicit methods' challenges with stiff systems. At each step of the simulation, an implicit algorithm solves a system of non-linear equations:

$$S_F(\vec{x}(t), \vec{y}(t), \vec{x}(t + \Delta t), \vec{y}(t + \Delta t), \eta) = 0 \quad (35)$$

$$S_G(\vec{x}(t), \vec{y}(t), \vec{x}(t + \Delta t), \vec{y}(t + \Delta t), \psi) = 0. \quad (36)$$

Newton's method is commonly used for the non-linear step in implicit methods; this reduces the process to a sequence of large linear system solves $Ax = b$ where A is of size $n \times n$ (n is the number of states). As a result, the computational complexity of an implicit method is dominated by the linear solution method, which is a function of the required precision and number of variables, with an upper bound $O(n^3)$. Several general-purpose integration algorithms use advanced stepping methods and parallel linear algebra libraries to reduce solution time in large stiff systems [53]. The non-linear solve requirements of this formulation increase the computational burden per time step, but it enables solving systems that are not numerically stable with explicit methods.

Simulation transformations and simplifications can avoid the need for implicit solvers by generating a non-stiff representation of an otherwise stiff system. For example, if a model complies with the conditions to use SPT it is possible to remove faster differential terms and reduce model stiffness. This technique has been used successfully in QSP simulation software to eliminate stator electromagnetic dynamics from generator models [39] as exemplified in Section IV.B. Reduced simulation models that can employ explicit methods and large step lengths will generally be several times faster than a stiff model solved with an implicit method.

3) *Fixed and variable time step*: The choice between fixed and variable time step solvers depends on the properties of the simulation model. Fixed-step integration methods use the same Δt throughout a simulation and are the only suitable alternative for time-variant models. As discussed in the previous section, decreasing Δt to increase accuracy also increases the simulation time. However, the accuracy of fixed time step approaches depends on the system properties and it does not imply that the integration error remains constant

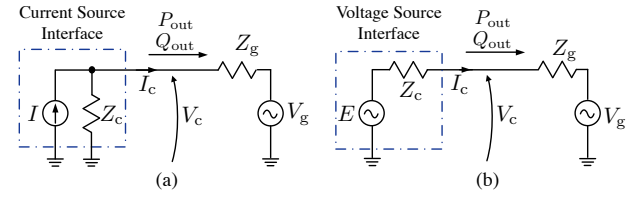


Fig. 6. Interface options of devices to an infinite bus V_g .

throughout the simulation [50]. As a result, in fixed-time step solvers, the step length is usually decreased to meet the most stringent accuracy requisites, which might only be required during a portion of the simulation and results in unnecessary computations.

When a simulation model is time-invariant, it is possible to employ variable-step solution methods. Variable-step solvers employ different techniques and heuristics to change the step size throughout the simulation to reduce computing time without compromising accuracy. For example, during fast dynamics, variable-step solvers decrease the step size, and as the system settles and slower dynamics dominate, the step size increases. Although it is possible that the calculation of suitable step length throughout the simulation (i.e., step rejection) increases the computational cost, the additional cost is presumed to be offset by performing a reduced number of steps. The effectiveness of variable time-step methods depends on the implementation details making it difficult to develop generalized guidelines for their use. However, there have been algorithmic innovations in the variable time step control field to reduce rejection; notably, the use of *PID* step-size control [54]. In practice, most commercial applications employ fixed time step methods for both EMT and QSP simulations, and adaptive time stepping is seldom used.

4) *Interfacing considerations*: Given the control flexibility encountered in IBR control, these sources can be modeled as “current source interface” with a large Norton impedance (see Fig. 6(a)) or as a “voltage source” using a Thevenin equivalent (see Fig. 6(b)). Although from the circuit perspective both models are equivalent, the interfacing modeling choice has implications for the numerical stability of the integration method.

When an IBR is modeled as a current source, the assumption is that the Norton equivalent current is the same as the network-injected current. Current injection models can lead to non-convergence in the integration method due to small diagonal entries in the diagonal of the admittance matrix from the inverse of IBRs Norton impedance. When the admittance matrix is close to the singularity, it is more difficult to solve the network voltages (i.e., $\vec{i} = \mathbf{Y}\vec{v}$). Furthermore, the Norton injected current would be a function of the voltage at the terminals, so there needs to be a convergence routine at each time step when differential equations and algebraic equations are solved sequentially. Additionally, in cases with a weak grid, the convergence steps might not converge in a reasonable number of iterations. On the other hand, if both systems of equations are solved simultaneously, convergence-related issues are reduced, but in extreme cases, the Newton

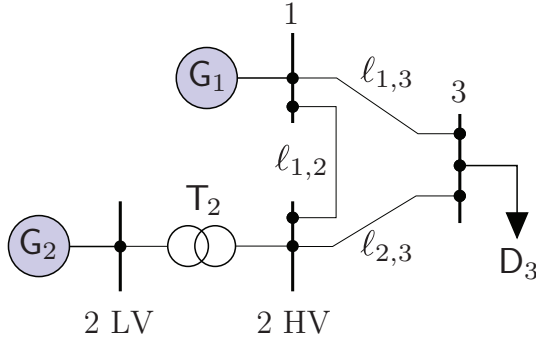


Fig. 7. Three-bus high-voltage (HV) network system motivating example.

iteration can also fail if it results in a Jacobian bad numerical conditioning.

It is typical for device models in commercial computational tools to be connected to the network using a Norton current-source equivalent (see Fig. 6). This is because inverter models are primarily designed for a current control representation. When the models have a “voltage source interface,” the inverter model is connected through a Thevenin impedance. However, this impedance is only included in the admittance matrix if the device model is changed to its Norton equivalent (see [55], [56] for details on the conversion between Norton and Thevenin equivalents). To improve numerical convergence, using Thevenin interfaced models and a current control representation is more appropriate, but this requires carefully constructed IBR control models.

D. Exemplifying simulation cases

This section showcases the simulation results of a line trip between buses 1 and 2 for a small IBR dominated system in Fig. 7 using three model formulations: waveform EMT, dq-EMT, and QSP. The objective is to showcase the dq-EMT equivalence with waveform simulations and demonstrate the effects of QSP simplifying assumptions. The network is modeled using a π -line, G_1 features a grid forming inverter with Virtual Synchronous Machine (VSM) control [57] and G_2 uses droop-control [5]. The QSP model formulation uses an algebraic representation of the electromagnetic circuits, lines, and inverter filters.

The QSP and dq-EMT simulations were conducted using the flexible formulation software `PowerSimulationsDynamics.jl` (PSID.jl), and the waveform simulation was conducted with PSCAD. The control blocks of the inverters are implemented as custom PSCAD components to match the models available in PSID.jl employing an ideal source output at the converter side of the filter.⁸ From the numerical standpoint, the dq-EMT model has a stiffness ratio of $\sigma = 2185$, whereas in the QSP case, $\sigma = 105$. The order of magnitude difference between stiffness ratios and evaluation steps demonstrates the implications of including electromagnetics in the average

model and the potential benefits of employing SPT in the model formulation.

The dq-EMT and QSP models employ the high-precision adaptive time step solver Rodas5 [58] with $\text{abstol} = 10^{-14}$ and $\text{reltol} = 10^{-14}$. The waveform EMT simulation is set to a $5\mu\text{s}$ fixed time-step. These values are used to guarantee that the comparisons are made at high accuracy levels. To emphasize the computational impacts of the transformation and simplifications, over a 10-second simulation the fixed-time-step method performed $2 \cdot 10^6$ evaluations, while the dq-EMT only required 31736 evaluations with time-steps in a range between $1.7\mu\text{s}$ and 7ms . However, only 18 of the 31736 were smaller than 1ms . On the other hand, the simplest QSP model only required 567 steps with time-steps in a range between $1\mu\text{s}$ to 0.1s making it the model with the least amount of evaluations required as expected given the discussion in Section IV.A

Figure 8 showcases the close match between dq and waveform solutions for the bus voltages and the capability of average models to capture EMT dynamics. The results also show that the QSP model does not capture high-frequency dynamics and has a slightly different trajectory. Figure 9 shows a comparison of the internal states of the PLL and outer control in the inverter with VSM control. These results display the effects of detailed electromagnetic modeling in the internal PLL and VSM states. The results showcase that the additional dynamics from the lines and the filter’s electromagnetics affect the VSM frequency estimation ω_{olc} , and in extreme cases, the oscillations could destabilize the controller. Further, both EMT models can reflect the oscillatory dynamics of the states $v_{d,\text{pll}}$ and $v_{q,\text{pll}}$, which demonstrates the equivalence between waveform and dq models for three-phase balanced systems.

VI. CONCLUDING REMARKS

We have made the case that the distinction between QSP and EMT models is insufficient to characterize the fundamentals of specific simulation models and techniques. Instead, as we reviewed in this paper, there is a large diversity of transformations and simplifications that yield a range of simulations models, each of which differently balances computational complexity with model fidelity—provided that certain operating conditions are met, such as narrow-band phenomena in dynamic phasors. Compared with a computationally expensive waveform simulation, these transformations enable cheaper EMT simulations without loss of information. Figure 2 and Table I summarize the proposed classification taxonomy for time-domain simulations.

This paper also showcases that the applicability of certain simplification techniques, like SPT, relies heavily on the control parameters of IBRs and the time constants of the remainder of the system. As a result, modeling requirements must be determined from a detailed model before any simplifications. This, in turn, affects the generalizability of specific device models and assumptions in different systems under different disturbances.

When selecting a simulation model and numerical method, the question to answer is: “What constitutes a valid solution?”

⁸The code to reproduce this experiment can be obtained at <https://github.com/Energy-MAC/SimulationModelsComparison.git>

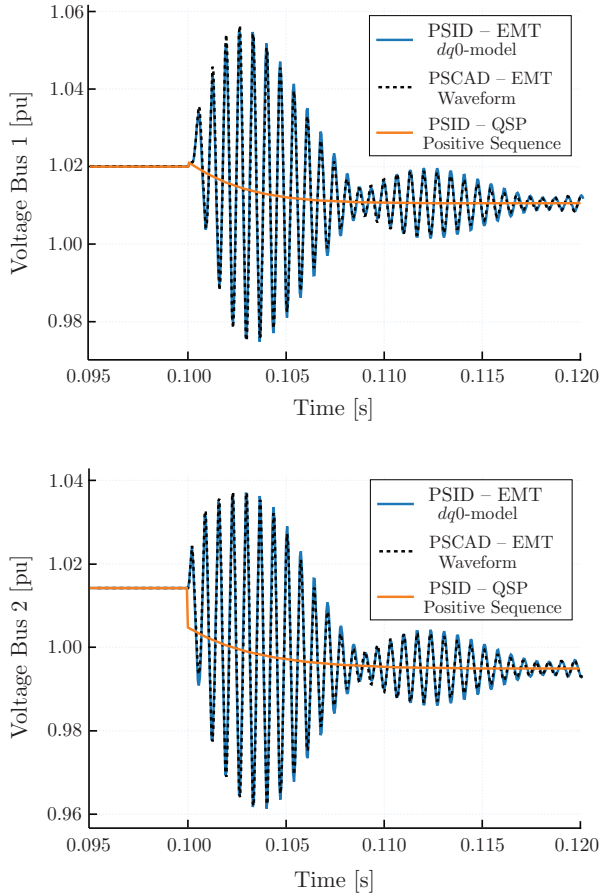


Fig. 8. Voltage magnitude transient response.

In some situations, the oscillatory behavior observed in Fig. 8 is not relevant to the analysis, and it might not be important to recover that information. This would be especially true over long simulation time spans. However, in other situations, information about high-frequency oscillation (such as its magnitude and energy) is highly relevant. This indicates a careful selection of which states to maintain and which ones to eliminate is critical. Finally, there will be situations like protection switching studies or transformer energizing where the waveform results will be required, and average models might not suffice to recover critical, very fast transient behavior.

Finally, we stress that for practitioners, the distinction between simulation models comes from the availability of a framework to solve such simulations. The lack of commercial software for novel simulation techniques hinders the exploration of novel alternatives that address existing approaches' shortcomings. Thus, research and development on time-domain simulation software are essential to analyzing, in a computationally efficient manner, the myriad IBRs architectures of future AC-DC hybrid power systems.

ACKNOWLEDGEMENTS

We thank C. Roberts, M. Bossart, G. Colon-Reyes, B.M. Hodge, and many others for fruitful discussions that led to the development of this paper. We thank M. Bossart for helping

implement the PSCAD simulations used in the example. This work was authored in part by the National Renewable Energy Laboratory, operated by Alliance for Sustainable Energy, LLC, for the U.S. Department of Energy (DOE) under Contract No. DE-AC36-08GO28308. Funding provided by U.S. Department of Energy's Office of Energy Efficiency and Renewable Energy under Solar Energy Technologies Office Agreement Number 33505. The views expressed in the article do not necessarily represent the views of the DOE or the U.S. Government. The U.S. Government retains and the publisher, by accepting the article for publication, acknowledges that the U.S. Government retains a nonexclusive, paid-up, irrevocable, worldwide license to publish or reproduce the published form of this work, or allow others to do so, for U.S. Government purposes.

REFERENCES

- [1] M. Paolone, T. Gaunt, X. Guillaud, M. Liserre, S. Meliopoulos, A. Monti, T. Van Cutsem, V. Vittal, and C. Vournas, "Fundamentals of power systems modelling in the presence of converter-interfaced generation," *Electric Power Systems Research*, vol. 189, p. 106811, 2020.
- [2] N. Hatziaargyriou, J. Milanovic, C. Rahmann, V. Ajjarapu, C. Canizares, I. Erlich, D. Hill, I. Hiskens, I. Kamwa, B. Pal *et al.*, "Definition and classification of power system stability revisited & extended," *IEEE Transactions on Power Systems*, 2020.
- [3] F. Milano, F. Dörfler, G. Hug, D. J. Hill, and G. Verbič, "Foundations and challenges of low-inertia systems," in *2018 Power Systems Computation Conference (PSCC)*. IEEE, 2018, pp. 1–25.
- [4] "IEEE guide for synchronous generator modeling practices and parameter verification with applications in power system stability analyses," *IEEE Std 1110-2019 (Revision of IEEE Std 1110-2002)*, pp. 1–92, 2020.
- [5] U. Markovic, O. Stanojev, P. Aristidou, E. Vrettos, D. S. Callaway, and G. Hug, "Understanding small-signal stability of low-inertia systems," *IEEE Transactions on Power Systems*, vol. 36, no. 5, pp. 3997–4017, 2021.
- [6] G. S. Misyris, S. Chatzivasileiadis, and T. Weckesser, "Grid-forming converters: Sufficient conditions for rms modeling," *Electric Power Systems Research*, vol. 197, p. 107324, 2021.
- [7] R. Henriquez-Auba, J. D. Lara, C. Roberts, and D. S. Callaway, "Grid forming inverter small signal stability: Examining role of line and voltage dynamics," in *IECON 2020 The 46th Annual Conference of the IEEE Industrial Electronics Society*. IEEE, 2020, pp. 4063–4068.
- [8] Q. Huang, D. Ramasubramanian, V. Vittal, B. Keel, and J. Silva, "Effect of accurate modelling of converter interfaced generation on a practical bulk power system," *IET Generation, Transmission & Distribution*, vol. 14, no. 15, pp. 3108–3116, 2020.
- [9] S. Subedi, M. Rauniyar, S. Ishaq, T. M. Hansen, R. Tonkoski, M. Shirazi, R. Wies, and P. Cicilio, "Review of methods to accelerate electromagnetic transient simulation of power systems," *IEEE Access*, vol. 9, pp. 89 714–89 731, 2021.
- [10] Y. Li, Y. Gu, and T. Green, "Mapping of dynamics between mechanical and electrical ports in SG-IBR composite grids," *IEEE Transactions on Power Systems*, pp. 1–1, 2022.
- [11] D. Venkatramanan, M. K. Singh, O. Ajala, A. Dominguez-Garcia, and S. Dhople, "Integrated system models for networks with generators & inverters," *arXiv preprint arXiv:2203.08253*, 2022.
- [12] R. Rosso, X. Wang, M. Liserre, X. Lu, and S. Engelken, "Grid-forming converters: Control approaches, grid-synchronization, and future trends—a review," *IEEE Open Journal of Industry Applications*, vol. 2, pp. 93–109, 2021.
- [13] K. Sano, S. Horiuchi, and T. Noda, "Comparison and selection of grid-tied inverter models for accurate and efficient emt simulations," *IEEE Transactions on Power Electronics*, vol. 37, no. 3, pp. 3462–3472, 2022.
- [14] V. A. Lacerda, E. P. Araujo, M. Cheah-Mañe, and O. Gomis-Bellmunt, "Phasor modeling approaches and simulation guidelines of voltage-source converters in grid-integration studies," *IEEE Access*, vol. 10, pp. 51 826–51 838, 2022.
- [15] A. Yazdani and R. Iravani, *Voltage-sourced converters in power systems: modeling, control, and applications*. John Wiley & Sons, 2010.
- [16] F. Milano and Á. O. Manjavacas, *Frequency Variations in Power Systems: Modeling, State Estimation, and Control*. John Wiley & Sons, 2020.

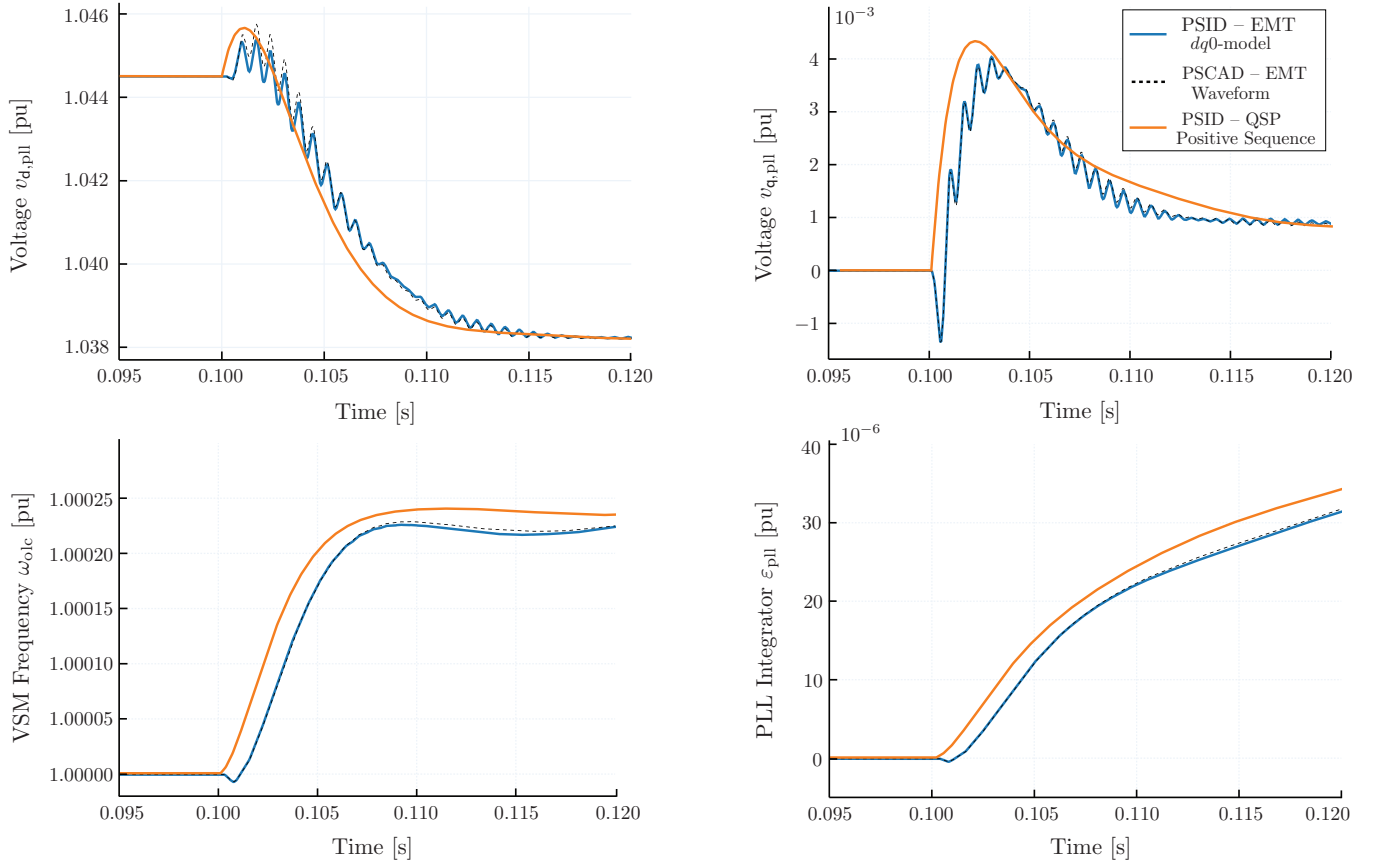


Fig. 9. Transient response for Inverter with VSM control

- [17] C. J. O'Rourke, M. M. Qasim, M. R. Overlin, and J. L. Kirtley, "A geometric interpretation of reference frames and transformations: dq0, clarke, and park," *IEEE Transactions on Energy Conversion*, vol. 34, no. 4, pp. 2070–2083, 2019.
- [18] H. K. Khalil, *Nonlinear systems; 3rd ed.* Upper Saddle River, NJ: Prentice-Hall, 2002.
- [19] S. Chiniforoosh, J. Jatskevich, A. Yazdani, V. Sood, V. Dinavahi, J. Martinez, and A. Ramirez, "Definitions and applications of dynamic average models for analysis of power systems," *IEEE Transactions on Power Delivery*, vol. 25, no. 4, pp. 2655–2669, 2010.
- [20] P. Zhang, J. R. Marti, and H. W. Dommel, "Synchronous machine modeling based on shifted frequency analysis," *IEEE Transactions on Power Systems*, vol. 22, no. 3, pp. 1139–1147, 2007.
- [21] S. R. Sanders, J. M. Noworolski, X. Z. Liu, and G. C. Verghese, "Generalized averaging method for power conversion circuits," *IEEE Transactions on power Electronics*, vol. 6, no. 2, pp. 251–259, 1991.
- [22] S. Sudhoff, K. Corzine, H. Hegner, and D. Delisle, "Transient and dynamic average-value modeling of synchronous machine fed load-commutated converters," *IEEE Transactions on Energy Conversion*, vol. 11, no. 3, pp. 508–514, 1996.
- [23] C. Demarco and G. Verghese, "Bringing phasor dynamics into the power system load flow," in *1993 North American Power Symposium Washington, D.C.*, 10 1993, pp. 463–729.
- [24] V. Venkatasubramanian, "Tools for dynamic analysis of the general large power system using time-varying phasors," *Int. Journal of Electrical Power & Energy Systems*, vol. 16, no. 6, pp. 365–376, 1994.
- [25] V. Venkatasubramanian, H. Schattler, and J. Zaborszky, "Fast time-varying phasor analysis in the balanced three-phase large electric power system," *IEEE Transactions on Automatic Control*, vol. 40, no. 11, pp. 1975–1982, 1995.
- [26] J. Marti, "Shifted frequency analysis (SFA) for EMT simulation of fundamental frequency power system dynamics," in *Internal Report, Power System Laboratory*. The University of British Columbia, 2005.
- [27] S. Haykin, *Communication systems*. John Wiley & Sons, 2008.
- [28] T. Demiray, "Simulation of power system dynamics using dynamic phasor models," Ph.D. dissertation, ETH Zurich, 2008.
- [29] J. Zaborszky, H. Schattler, and V. Venkatasubramanian, "Error estimation and limitation of the quasi stationary phasor dynamics," in *Proc. Power Syst. Comput. Conf.*, 1993, pp. 721–729.
- [30] P. J. Hart, J. Goldman, R. H. Lasseter, and T. M. Jahns, "Impact of harmonics and unbalance on the dynamics of grid-forming, frequency-droop-controlled inverters," *IEEE Journal of Emerging and Selected Topics in Power Electronics*, vol. 8, no. 2, pp. 976–990, 2019.
- [31] A. Stankovic, S. Sanders, and T. Aydin, "Dynamic phasors in modeling and analysis of unbalanced polyphase ac machines," *IEEE Transactions on Energy Conversion*, vol. 17, no. 1, pp. 107–113, 2002.
- [32] C. L. Fortescue, "Method of symmetrical co-ordinates applied to the solution of polyphase networks," *Transactions of the American Institute of Electrical Engineers*, vol. XXXVII, no. 2, pp. 1027–1140, 1918.
- [33] R. H. Park, "Two-reaction theory of synchronous machines generalized method of analysis-part I," *Transactions of the American Institute of Electrical Engineers*, vol. 48, no. 3, pp. 716–727, 1929.
- [34] J. Belikov and Y. Levron, "Comparison of time-varying phasor and dq0 dynamic models for large transmission networks," *International Journal of Electrical Power & Energy Systems*, vol. 93, pp. 65–74, 2017.
- [35] F. Milano, "Complex frequency," *IEEE Transactions on Power Systems*, pp. 1–1, 2021.
- [36] B. Stott, "Power system dynamic response calculations," *Proceedings of the IEEE*, vol. 67, no. 2, pp. 219–241, 1979.
- [37] J. H. Chow, G. Peponides, P. Kokotovic, B. Avramovic, and J. Winkelman, *Time-scale modeling of dynamic networks with applications to power systems*. Springer, 1982, vol. 46.
- [38] P. Kokotović, H. K. Khalil, and J. O'reilly, *Singular perturbation methods in control: analysis and design*. SIAM, 1999.
- [39] P. Sauer, S. Ahmed-Zaid, and P. Kokotovic, "An integral manifold approach to reduced order dynamic modeling of synchronous machines," *IEEE transactions on Power Systems*, vol. 3, no. 1, pp. 17–23, 1988.
- [40] P. W. Sauer, M. A. Pai, and J. H. Chow, *Power system dynamics and stability: with synchrophasor measurement and power system toolbox*. John Wiley & Sons, 2017.
- [41] H. W. Dommel, "Digital computer solution of electromagnetic transients

- in single- and multiphase networks,” *IEEE transactions on power apparatus and systems*, no. 4, pp. 388–399, 1969.
- [42] L. Petzold, “Differential/algebraic equations are not ode’s,” *SIAM Journal on Scientific and Statistical Computing*, vol. 3, no. 3, pp. 367–384, 1982.
 - [43] D. Baimel, J. Belikov, J. M. Guerrero, and Y. Levron, “Dynamic modeling of networks, microgrids, and renewable sources in the dq0 reference frame: A survey,” *IEEE Access*, vol. 5, pp. 21 323–21 335, 2017.
 - [44] P. Pourbeik, J. J. Sanchez-Gasca, J. Senthil, J. D. Weber, P. S. Zadehkhosht, Y. Kazachkov, S. Tacke, J. Wen, and A. Ellis, “Generic dynamic models for modeling wind power plants and other renewable technologies in large-scale power system studies,” *IEEE Transactions on Energy Conversion*, vol. 32, no. 3, pp. 1108–1116, 2017.
 - [45] B. Johnson, T. G. Roberts, O. Ajala, A. Domínguez-García, S. Dhople, D. Ramasubramanian, A. Tuohy, D. Divan, and B. Kroposki, “A generic primary-control model for grid-forming inverters: Towards interoperable operation & control,” in *Proc. Hawaii Int. Conf. System Sciences*, 2022.
 - [46] D. Ramasubramanian, W. Wang, P. Pourbeik, E. Farantatos, A. Gaikwad, S. Soni, and V. Chadliev, “Positive sequence voltage source converter mathematical model for use in low short circuit systems,” *IET Generation, Transmission & Distribution*, vol. 14, no. 1, pp. 87–97, 2020.
 - [47] L. Luo and S. V. Dhople, “Spatiotemporal model reduction of inverter-based islanded microgrids,” *IEEE Transactions on Energy Conversion*, vol. 29, no. 4, pp. 823–832, 2014.
 - [48] O. Ajala, M. Lu, S. Dhople, B. B. Johnson, and A. Dominguez-Garcia, “Model reduction for inverters with current limiting and dispatchable virtual oscillator control,” *IEEE Transactions on Energy Conversion*, pp. 1–1, 2021.
 - [49] J. A. Martinez-Velasco, *Transient analysis of power systems: solution techniques, tools and applications*. John Wiley & Sons, 2014.
 - [50] F. E. Cellier and E. Kofman, *Continuous system simulation*. Springer Science & Business Media, 2006.
 - [51] N. Watson and J. Arrillaga, *Power systems electromagnetic transients simulation*. Iet, 2003, vol. 39.
 - [52] R. Concepcion, R. Elliott, M. Donnelly, and J. Sanchez-Gasca, “On extended-term dynamic simulations with high penetrations of photovoltaic generation,” in *2016 IEEE Power and Energy Society General Meeting (PESGM)*. IEEE, 2016, pp. 1–5.
 - [53] A. Bojańczyk, “Complexity of solving linear systems in different models of computation,” *SIAM Journal on Numerical Analysis*, vol. 21, no. 3, pp. 591–603, 1984.
 - [54] K. Gustafsson, “Control-theoretic techniques for stepsize selection in implicit runge-kutta methods,” *ACM Transactions on Mathematical Software (TOMS)*, vol. 20, no. 4, pp. 496–517, 1994.
 - [55] C. Li, Y. Wu, H. Zhang, H. Ye, Y. Liu, and Y. Liu, “Steps: A portable dynamic simulation toolkit for electrical power system studies,” *IEEE Transactions on Power Systems*, vol. 36, no. 4, pp. 3216–3226, 2021.
 - [56] P. Siemens, “PSSe program operation manual.” Siemens, 2017.
 - [57] S. D’Arco, J. A. Suul, and O. B. Fosso, “A virtual synchronous machine implementation for distributed control of power converters in smartgrids,” *Electric Power Systems Research*, pp. 180–197, 2015.
 - [58] C. Rackauckas and Q. Nie, “Differential equations. jl—a performant and feature-rich ecosystem for solving differential equations in julia,” *Journal of open research software*, vol. 5, no. 1, 2017.

José Daniel Lara (Senior Member, IEEE) received the B.Sc. and Licenciatura degrees in electrical engineering from the University of Costa Rica, San Pedro, Costa Rica, in 2009 and 2012, respectively, the M.Sc. degree in Electrical and Computer Engineering from the University of Waterloo, Waterloo, ON, Canada, in 2014, M.S. in Energy and Resources with focus on Engineering and Business for Sustainability in 2017, and Ph.D. in Energy and Resources with Designated Emphasis in Computational and Data Science and Engineering from the University of California, Berkeley, CA, USA in 2022. He currently works at the National Renewable Energy Laboratory (NREL) with the Grid Planning and Analysis Center (GPAC). His research interests include the analysis and simulation of power systems and their applications to power systems operation and quantitative energy policy.

Rodrigo Henriquez-Auba (Member, IEEE) received the B.Sc. and M.Sc. in electrical engineering from the Pontifical Catholic University of Chile, Santiago, Chile, in 2014 and 2016, respectively, and the Ph.D. degree in Electrical Engineering and Computer Sciences from the University of California, Berkeley, CA, USA, in 2022. He currently works at the National Renewable Energy Laboratory (NREL) and his research interests include operation and planning of electric systems with large shares of renewable sources, and control, modeling and simulation of power systems and power electronics.

Deepak Ramasubramanian (Senior Member, IEEE) received the B.E. degree from the PES Institute of Technology, Bangalore, KA, India, in 2011, and the M.Tech. degree from the Indian Institute of Technology Delhi, New Delhi, India, in 2013 and Ph.D. degree at Arizona State University, Tempe, AZ, USA in 2017. Deepak is a Technical Leader in the Grid Operations and Planning Group at EPRI and leads research projects related to modeling of inverter-based resources for bulk power system analysis.

Sairaj Dhople (Senior Member, IEEE) received the B.S., M.S., and Ph.D. degrees in electrical engineering from the University of Illinois at Urbana-Champaign, Urbana, IL, USA, in 2007, 2009, and 2012, respectively. He is currently Robert & Sydney Anderson Associate Professor with the Department of Electrical and Computer Engineering, University of Minnesota, Minneapolis, MN, USA. His research interests include modeling, analysis, and control of power electronics and power systems with a focus on renewable integration. Dr. Dhople is the recipient of the National Science Foundation CAREER Award in 2015, the Outstanding Young Engineer Award from the IEEE Power and Energy society in 2019, and the IEEE Power and Energy Society Prize Paper Award in 2021.

Duncan S. Callaway (Member, IEEE) is an Associate Professor of Energy and Resources at the University of California, Berkeley. He is also a faculty affiliate in Electrical Engineering and Computer Science, and a faculty scientist at Lawrence Berkeley Laboratory. He received his PhD from Cornell University. He has held engineering positions at Davis Energy Group and PowerLight Corporation, and academic positions at UC Davis, the University of Michigan and UC Berkeley. Duncan teaches courses on electric power systems and at the intersection of statistical learning and energy. His research focuses on grid integration of renewable electricity, and models and control strategies for power system dynamics, demand response, electric vehicles and electricity storage.

Seth Sanders (Fellow, IEEE) received the S.B. degree in electrical engineering and physics in 1985, and the S.M. and Ph.D. degrees in electrical engineering from the Massachusetts Institute of Technology, Cambridge, MA, USA, in 1985 and 1989, respectively. He is currently a Professor with the Department of Electrical Engineering and Computer Sciences, University of California, Berkeley, CA, USA, and co-founder and Chief Technology Officer with Amber Kinetics, a Technology Developer and manufacturer of utility scale flywheel energy storage systems. Following an early experience as a Design Engineer with the Honeywell Test Instruments Division from 1981 to 1983, he joined the UC Berkeley faculty in 1989. His technical interests are broadly in electrical energy and power conversion systems. He is presently or has recently been active in supervising research projects in the areas of renewable energy systems, high frequency integrated power conversion circuits, IC designs for power conversion applications, and electric machine systems. During the 1992–1993 academic year, he was on industrial leave with National Semiconductor, Santa Clara, CA. Dr. Sanders was the recipient of the NSF Young Investigator Award and multiple Best Paper Awards from the IEEE Power Electronics and IEEE Industry Applications Societies, and IEEE PELS Modeling and Control Technical Achievement Award. He was the Chair of the IEEE PELS Technical Committee on Computers in Power Electronics, Chair of the IEEE PELS Technical Committee on Power Conversion Components and Systems, and as Member-At-Large of the IEEE PELS Adcom. He is a past Distinguished Lecturer of the IEEE PELS and IAS societies.